Chen, You-Cheng; Chan, Hsun-Chuan; Jia, Ya-Fei

Simulation of Vegetation Patch on Momentum and Mass Transports of Flow and Sediment in an Experimental Channel by Using CCHE 3D

12th International Conference on Hydroscience & Engineering
Hydro-Science & Engineering for Environmental Resilience
November 6-10, 2016, Tainan, Taiwan.

Simulation of Vegetation Patch on Momentum and Mass Transports of Flow and Sediment in an Experimental Channel by Using CCHE 3D

You-Cheng Chen[1], Hsun-Chuan Chan[1], Ya-Fei Jia[2]
1. National Chung Hsing University Department of Soil and Water Conservation
Taichung, Taiwan
2. National Center for Computational Hydroscience and Engineering
Mississippi, America

ABSTRACT

This study discusses the effects of vegetation communities on flow fields and river bed erosion with a numerical model CCHE 3D and presents the results of lab experiments. In the numerical model, the drag resulting from vegetation is considered with momentum equations, the physical properties of river streams are calculated with the mixing length turbulence modeling, and the changes to a river bed are calculated with reference to sediment transport experiences that simulate the effects of vegetation communities.

KEY WORDS: Turbulent flow; Numerical modeling; Vegetation; Sediment transport .

INTRODUCTION

Plant communities can change the flows and channels of rivers and ecologically diversify river environments. When plants reduce the flow velocity of streams and stabilize beds and banks, those plants facilitate the building of ecological habitats; however, plants also constrict streams and increase flow velocity and bed erosion. River vegetation is a double-edged sword that always is crucial to the sustainable management of rivers. Different vegetation types like herbs, shrubs, and arbors have different effects on river channels. Local land management controversies, including construction safety and habitat management, require extensive information about river dynamics. As a reference, one can use a roughness coefficient to assess the vegetation in a river's environment, but that provides insufficient information for such controversies.

When plants are submerged in a river, they can be considered as roughness elements and modeled by roughness coefficients (Vionnet et al., 2004.) The present study investigates the effects of groups of emergent woody plants on river flow and sediment transport. The findings of the present study pertain to emergent woody plants; the flow in the channel with such a vegetation group can be modeled as passing through a cylinder group with a different arrangement. Nehal and Yan (2005) conducted an experiment and indicated that the flow resistance relates to the vegetation group density, and the Manning roughness coefficient changes with the water depth. In this study, groups of woody plants are considered to be emergent, and the flow near the vegetation zone is modeled as a highly three-dimensional phenomenon. A three-dimensional numerical model, was written in CCHE 3D, and groups of plants were simulated in greater detail than would be possible with simple roughness calculations. A laboratory experiment was carried out and the physical results were compared to the simulation results.

In addition to flow, this study considers sediment transport. Sediment deposition is affected by particle size and river conditions. Lisle (1982) reported that, after flooding, sediment deposition reduces the roughness of a river channel, and improves the sediment transport. Laursen (1952) used the difference between inflow and outflow sediment carrying rates to calculate a river bed sediment scouring rate. He also reported that when the scour depth and water cross section increase, scouring rate decreases and converges to a constant. Sediment transport has been researched for years, but the interaction of vegetation and scour still eludes simplistic explanations. Therefore this study discusses the complex and complicated effects of vegetation groups on bed scour.

CCHE 3D Model

The CCHE 3D Model was developed at the National Center for Computational Hydroscience and Engineering of the University of Mississippi School of Engineering. This three-dimensional model enables simulation of steady and unsteady free surface turbulent flows and sediment transport. It had been used to analyze highly turbulent near field and natural river flows. An efficient element method was devised by modifications to the finite element method based on the collocation approach (Mayerlye et al., 1995); this efficient element method was employed for solving the Navier-Stokes equations and the free surface kinematics equation.

The unsteady, 3D Navier-Stokes equations could be expressed as Reynolds-averaged momentum equations and a continuity equation:

$$\frac{\partial u_i}{\partial t} + u_j \frac{\partial u_i}{\partial x_j} = -\frac{1}{\rho}\frac{\partial p}{\partial x_i} + \frac{\partial}{\partial x_j}\left(\nu \frac{\partial u_i}{\partial x_j} - \overline{u_i' u_j'}\right) + f_i \quad (1)$$

$$\frac{\partial u_i}{\partial x_i} = 0 \quad (2)$$

In Eqs. 1 and 2, u_i represent the velocity magnitudes of different directions, i = 1, 2, 3 correspond to x, y, z axes in a Cartesian coordinate system, and $u_i = u, v, w$; u_i' are velocity fluctuations; $-\overline{u_i' u_j'}$ are Reynolds stresses; p is pressure including both hydrostatic pressure p_h and nonhydrostatic pressure p_d ; ρ is fluid density; ν is fluid

kinematic viscosity; and f_i are body force terms. The free surface kinematics equation is used to describe the motion of the free surface, and it can be expressed as:

$$\frac{\partial \eta}{\partial t} + u_s \frac{\partial \eta}{\partial x} + v_s \frac{\partial \eta}{\partial y} - w_s = 0 \tag{3}$$

where η and subscript s give the free surface elevation and the velocity components at the free surface, respectively. Based on Boussinesq's assumption, the turbulence term in the momentum equations can be expressed as:

$$\tau_{ij} = -\overline{u_i' u_j'} = \nu_t (u_{i,j} + u_{j,i}) \tag{4}$$

where ν_t is eddy viscosity; τ_{ij} is the Reynolds shear stress. This model provides several approaches for estimating the eddy viscosity including: parabolic eddy viscosity distribution, mixing length eddy viscosity, wind induced eddy viscosity, and k-ε model. In this application, mixing length eddy viscosity is adopted:

$$\nu_t = l^2 \sqrt{\left(\frac{\partial u_i}{\partial x_j} + \frac{\partial u_j}{\partial x_i}\right) \frac{\partial u_i}{\partial x_j}} \tag{5}$$

$$l = \kappa z \sqrt{1 - \frac{z}{h}} \tag{6}$$

In Eqs. 5 and 6, l is the mixing length of vortex; κ is the Von Karman constant; z is the distance from the bed; h is the water depth.

Bed form change due to the interactions of vegetation, water, and sediment can be calculated by a sediment transport model based on nonequilibrium sediment transport. The discriminating factor that decides whether the bed is being scoured is the difference between the bed shear stress and the critical shear stress; when the bed shear stress is sufficiently high, it causes sediment to move. With reference to Jia and Wang (2001), this model uses two methods to calculate the bed shear stress; one is the log law expressed as:

$$\frac{u}{u^*} = \frac{1}{\kappa} \ln\left(E \frac{z u^*}{\nu}\right) \tag{7}$$

$$u^* = \sqrt{\frac{\tau}{\rho}}. \tag{8}$$

where u^* is shear velocity; E is the coefficient of roughness; τ is shear stress. The other method uses the bed roughness coefficient to calculate the bed shear stress components and the shear velocity:

$$\tau_{bi} = \frac{1}{h^{1/3}} \rho g n^2 u_i U \tag{9}$$

$$u^* = \sqrt{\left(\sum \tau_{bi}^2\right)/\rho}. \tag{10}$$

where τ_{bi} is the component of the bed shear stress; n is the Manning roughness coefficient.

After sediment starts to move, the bed load transport rate can be estimated by the nonequilibrium model that Wu et al. (2000) calculated as:

$$\frac{\partial(\delta \bar{c}_{bk})}{\partial t} + \frac{\partial(q_{bkx})}{\partial x} + \frac{\partial(q_{bky})}{\partial y} + \frac{1}{L_b}(q_{bk} - q_{b*k}) = 0 \tag{11}$$

where δ is the thickness of the bed load layer; $\bar{c}_{bk}$ is the concentration of the bed load for a specific particle size k; q_{bkx} and q_{bky} are the actual bed load transport rates for a specific particle size k; q_{b*k} is the equilibrium capacity bed load transport rate for a specific particle size k; L_b is the adaptation length of the bed load. Considering the mass conservation, the bed load exchange model near the bed can be written as:

$$(1 - p') \frac{\partial(z_{bk})}{\partial t} = \frac{1}{L_b}(q_{bk} - q_{b*k}) = 0 \tag{12}$$

where p' is the sediment porosity. Furthermore, sediment transport causes a scour hole to appear, and then the interaction between flow and sediment is strongly affected by vertical flows normal to the bed. The sediment entrainment in a scour hole is related to the turbulence caused by the vertical flow, which is termed intruding fluctuation (Jia et al., 2013.) Therefore the total effective shear stress for sediment entrainment, including the vertical impact effect, can be expressed as:

$$u_{*e} = u_{*\parallel} + u_{*l} \tag{13}$$

This means the modified total effective shear stress is equal to $u_{*\parallel}$, the shear stress computed using the near bed flow parallel to the bed, plus u_{*l}, the intruding shear stress which can be approximated by:

$$u_{*l} \approx 0.456 C_s \sqrt{\overline{k_R} |R_\perp|} \tag{14}$$

where C_s is a calibration coefficient; $\overline{k_R}$ is the depth-averaged turbulence energy in the scour hole bed surface; $R_\perp$ is a nondimensional scale for evaluating the magnitude of the available near bed turbulence energy that impinges into the near bed sediment layer and triggers additional sediment motion. The modified shear stress is used for enhancing the accuracy of the flow mechanism simulation, and for enhancing the accuracy of the sediment transport simulation.

The computational mesh generation corresponds to the experimental setup. The digital experimental channel model of the case with vegetated density equal to 0.05 is shown as Fig. 1. The mesh size is equal to 257 × 296.

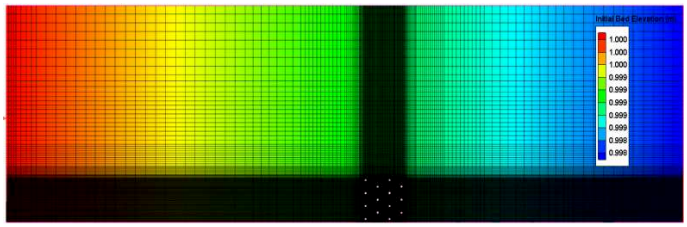

Φ = 0.05

Fig. 1 Digital experimental channel model

Physical Model Experiment Setup

The experiments were carried out in a water-recirculating flume with vegetation simulated by steel rods (Fig. 2.) The flume was 20 m long, 1 m wide, 0.6 m deep, and tilted at a constant slope of 0.001. The experiment reach was a sink that was installed at the center of the flume with 0.59 m sag.

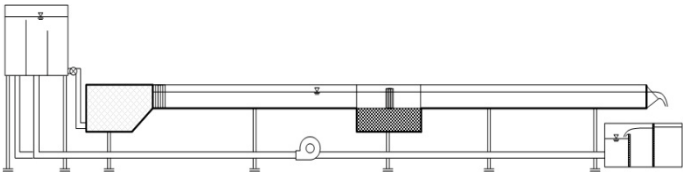

Fig. 2 Schematic diagram of flume

The sink was filled with uniform sand, which was 0.85 mm in grain diameter. The flow discharge was kept constant at 0.047 cms and the flow depth was 0.162 m. The simulated group of plants was constructed from cylindrical steel rods, which were 6.35 mm in diameter, and uniformly placed in a 0.1 m × 0.1 m patch on a perforated steel board. The vegetation zone was adjacent to a side wall of the experiment reach, and was constructed with $\Phi = 0.05$. For the coordinate system employed, x = 0 was located at the front edge of the vegetation zone, y = 0 was the flume wall of the groin side of the flume, and z = 0 was at the initial bottom level of the flume. The velocity distributions and the topography of bed form were measured by using acoustic velocimeter and laser distance meter.

RESULTS AND DISCUSSIONS

The flow field was controlled under the critical condition of sediment incipient motion. By passing through the vegetation zone, cross section constriction caused local flow velocity to accelerate. Local scour occurred.

Depth-average velocity distribution

Fig. 3a shows cross-sectional measurements taken 35 cm upstream from the vegetation zone. During the physical experiments, the flow was close to uniform flow, but the side wall effect caused the flow to lose a small amount of velocity. The solid line is the simulation result, and the starred line is the physical measurement. Fig. 3b shows cross-sectional measurements taken 3 cm upstream from the vegetation zone, and the simulated plants are shown in the figure. A reduction of flow velocity just in front of the vegetation zone can be observed, and increased velocity in the free zone that was not blocked by plants. This caused part of the flow to veer toward the center of the channel. The flow directly entering the vegetation zone decelerated, as shown in Figs. 3c, 3d. Generally, the peaks of the velocity occurred at the intervals between the plants, and the valleys were just downstream from the backs of plants, but they were shifted toward the free zone by the interactions of several rows of plants.

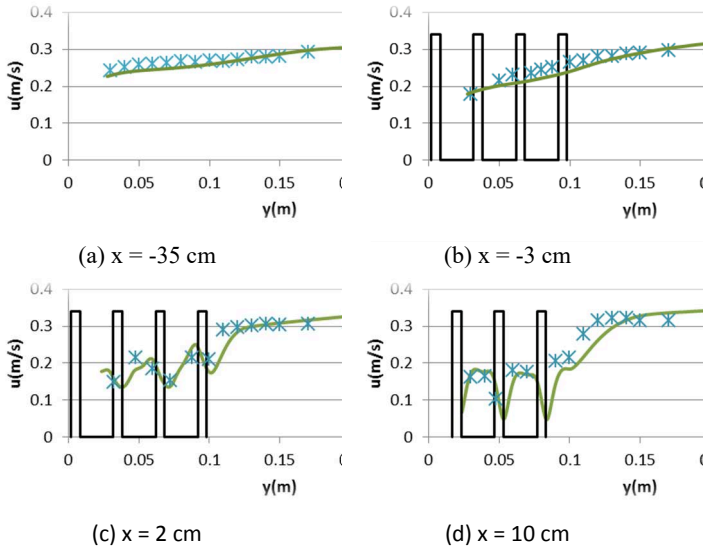

Fig. 3 Depth-average velocity distribution

Bed shear stress

The bed shear stress distribution for the run with $\Phi = 0.05$ is shown as Fig. 4. The shear stress in the u direction leads by longitudinal flow. Since it is the main flow direction, the u component is larger than other two direction components. Where the flow is blocked by plants, the flow in front of those plants has smaller shear velocity, and causes smaller bed shear stress. Some values are even negative (i.e., the direction is upstream). The values of bed shear stress are also negative in the recirculation zone behind the plants. The flow exhausted from the vegetation zone converges to the main flow. That convergence increases the shear velocity and the bed shear stress on the edge of the vegetation zone. The bed shear stress distribution beyond the y = 14 cm boundary is out of the influence of the vegetation zone, but the shear velocity and the shear stress are relatively low in the redeveloped boundary layer behind the vegetation zone. The v component shows that the flow veers as it is divided into two parts by each plant, which increases the shear stress for both sides of each plant. For each plant, the recirculation of the v component is not absolutely longitudinal or lateral, but takes values between both. The values of shear stress are negative in these areas, which implies the direction of shear stress is toward the wall. Part of the flow veers vertically, so that the w component of bed shear stress has a negative value. The kinematic energy of the flow intrudes into the bed of the channel because of the downward shear stress. The influence of downward shear stress on scour is more direct. The flow creates a vortex, and brings an upward jet flow after merging by passing through the plants, which tosses the sediment. Regarding sediment entrainment, the distance caused by shear stress is greater than the distance caused by flow. Total bed shear stress shows the largest value is not at the upstream corner, but by the side of the vegetation zone. In the vegetation zone, the largest bed shear stress is observed between the third row and the fourth row.

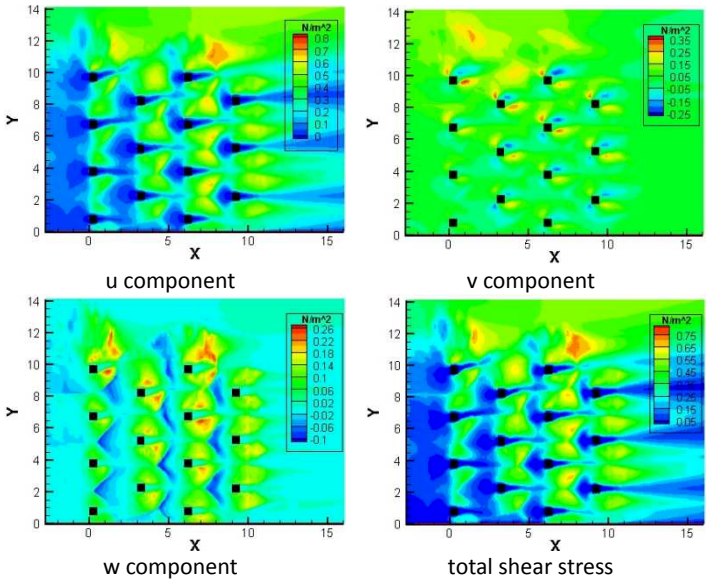

Fig. 4 Bed shear stress for the $\Phi = 0.05$ case

Final bed form

The experimental run with $\Phi = 0.05$ was maintained for 120 hours to ensure both transport and deposition reached equilibrium and the bed

form was stable. The result is shown as Fig. 5. The scour hole extends upstream about 3 cm from the vegetation zone. The largest scour depth is in the vegetation zone and between the second row and third row, and the value is 2.31 cm. The scour hole develops along the direction of the veered flow, which is from interior toward the diagonally back of the vegetation zone. The trend of the development corresponds to the bed shear stress distribution in Fig. 4. It goes out of the vegetation zone from the third row and moves back diagonally. The minimum velocity is in the recirculation zone behind the vegetation zone. The flow's sediment-carrying capacity is reduced and the flow deposits sediment behind the vegetation zone. The highest deposition can reach 1.8 cm. The upstream side of the deposition is mild and downstream side is steep. The deposition extends downstream to y = 10 cm, which is the boundary of the recirculation zone.

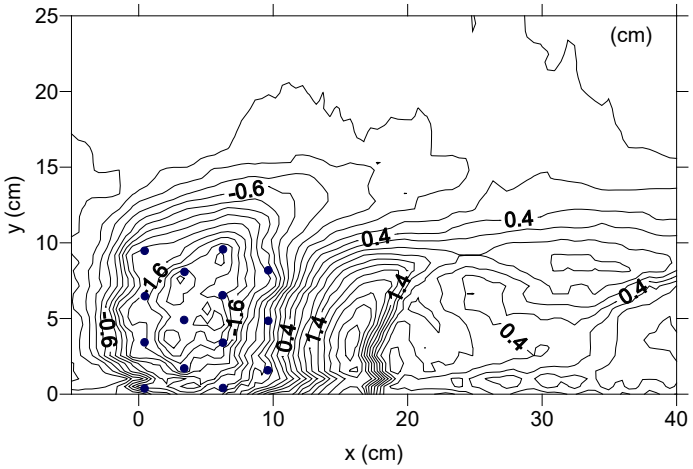

Fig. 5 Final topography for the Φ = 0.05 case

CONCLUSIONS

The two-dimensional numerical model allows a quick overview of the whole flow field. The three-dimensional velocity distribution and the flow structure near the obstructions are too complicated for the two-dimensional numerical model to describe. In the experimental case of a simulated vegetation zone with solid density of 0.05, the obstruction brings out vortexes when the flow directly goes through the vegetation zone, and causes part of the flow to veer to the free zone. Vertical flows include flows that are blocked by plants and turned vertical, and the horseshoe vortex merging behind plants and becoming an upward jet flow. These details can be only simulated by a three-dimensional numerical model, which can also cover spaces near boundaries where water surfaces cannot be easily measured.

In the case which Φ = 0.05, the models predicts the depth-average velocity distribution accurately. The constriction effect and the vortexes caused by the vegetation blockage tend to disorder the flow structure and reflect on the bed shear stress. The flow through the vegetation zone causes vertical flows and vortexes and increases local bed shear stress. A small part of the flow is extracted out of the vegetation zone and merges into main flow, which increases bed shear stress along the edge of the vegetation zone.Scour depth in the case of permeable vegetation group, the flow enters the vegetation zone and most of the flow goes through it, and even though only a small part of the flow is veered out, but the sediment-carrying capacity of the flow is much smaller.

Regarding the mesh size for numerical simulation, it must contain enough grids for each plant and each interval between two plants to present the flow structure. Due to the experimental channels are much smaller than real rivers. Using a dense mesh for a laboratory scale investigation requires consideration of short lengths inside the grids, and correspondingly small steps of time. In this study, the time step is 0.001 second, and therefore the computational effort required for simulation is immense. The simulation requires several times the duration of the physical experiment. However, if this model is applied to field scale problems, the time step can be increased, and the problem of excessive computational effort will no longer exist.

REFERENCES

Jia, Y, and Sam S.Y. Wang, (2001), Technical Manual of CCHE2D V2.0. NCCHE-TR-01-2, The University of Mississippi.

Jia, Y., M. Altinakar., M.S. Guney, A.O., Aksoy, and G. Bombar (2013), 3D Numerical Simulations Of Local Scouring Around Bridge Piers Under Non-Uniform Sediment Conditions. The 35th Congress of International Association for Hydraulic Research (IAHR), Sep.8-13, Chengdu China (CD-ROM).

Laursen, E. M. (1952). Observations on the nature of scour. Proc. 5th Hydr. Conf., University of Iowa, Iowa City, Iowa, 179-197

Lisle, T. E. (1982). Effects of aggradation and degradation on riffle-pool morphology in natural gravel channels. Water Resour. Res., 18, pp.1643-1651.

Mayerle, R., Toro, F. M., and Wang, S. S. Y., (1995). Verification of a three dimensional numerical model simulation of the flow in vicinity of spur dikes. J. Hydraul. Res., 33(2), 243-256.

Nehal, L. and Z. M. Yan (2005). Study on the flow of water through non-submerged vegetation. Proceedings of Hydrology Days 2005, 170-179.

Vionnet, C. A., P. A. Tassi and Martín Vide J. P. (2004). Estimates of flow resistance and eddy viscosity coefficients for 2D modelling on vegetated floodplains. Hydrological Processes, 18, 2907-2926.

Wu, W., S.S.Y. Wang, and Y. Jia. (2000). Nonuniform sediment transport in alluvial rivers. J. Hydr. Res., IAHR, 38(6), 427-434